TU/e EINDHOVEN UNIVERSITY OF TECHNOLOGY

Computational issues in time-dependent deformation and fracture of concrete

Citation for published version (APA):
Borst, de, R., Boogaard, van den, A. H., Sluys, L. J., & Bogert, van den, P. A. J. (1993). Computational issues in time-dependent deformation and fracture of concrete. In Z. P. Bazant, & I. Carol (Eds.), *Creep and shrinkage of concrete : proceedings of the fifth international RILEM symposium, Barcelona, Spain, September 6-7, 1993* (pp. 309-326). (RILEM proceedings; Vol. 22). E&FN SPON.

Document status and date:
Published: 01/01/1993

Document Version:
Publisher's PDF, also known as Version of Record (includes final page, issue and volume numbers)

Please check the document version of this publication:

• A submitted manuscript is the version of the article upon submission and before peer-review. There can be important differences between the submitted version and the official published version of record. People interested in the research are advised to contact the author for the final version of the publication, or visit the DOI to the publisher's website.
• The final author version and the galley proof are versions of the publication after peer review.
• The final published version features the final layout of the paper including the volume, issue and page numbers.

Link to publication

General rights
Copyright and moral rights for the publications made accessible in the public portal are retained by the authors and/or other copyright owners and it is a condition of accessing publications that users recognise and abide by the legal requirements associated with these rights.

• Users may download and print one copy of any publication from the public portal for the purpose of private study or research.
• You may not further distribute the material or use it for any profit-making activity or commercial gain
• You may freely distribute the URL identifying the publication in the public portal.

If the publication is distributed under the terms of Article 25fa of the Dutch Copyright Act, indicated by the "Taverne" license above, please follow below link for the End User Agreement:

www.tue.nl/taverne

Take down policy
If you believe that this document breaches copyright please contact us at:

openaccess@tue.nl

providing details and we will investigate your claim.

Download date: 04. Oct. 2023

39 COMPUTATIONAL ISSUES IN TIME-DEPENDENT DEFORMATION AND FRACTURE OF CONCRETE

(Principal Lecture)

R. de BORST
Delft University of Technology/TNO Building and Construction Research, The Netherlands
A. H. van den BOOGAARD
TNO Building and Construction Research, The Netherlands
L. J. SLUYS
Delft University of Technology, Delft, The Netherlands
P. A. J. van den BOGERT
Shell Research B.V., The Netherlands

Abstract

Creep formulations for concrete that are amenable to an efficient numerical implementation are reviewed. Both short-term and long-term creep processes are addressed. An elegant formulation is derived for the use of smeared-crack models in finite element analyses of time-dependent (viscous) deformations and is shown to yield realistic simulations of crack patterns. Possible consequences of the inclusion of rate-effects on the well-posedness of rate boundary value problems that involve smeared cracking and tension softening are discussed. Finally, an automatic scheme for selecting the time step in numerical computations is presented.

Keywords: Creep, Visco-Elasticity, Fracture, Finite Element Analysis

1 Introduction

Creep and cracking are among the most prominent non-linear phenomena that affect serviceability of concrete structures, either plain, reinforced or prestressed. As a result much attention has been devoted to developing accurate constitutive models for the long-term behaviour of concrete (*cf.* Bazant *et al.* 1988 for a review). Almost invariably, these models find their point of departure in the linear theory of visco-elasticity. A basic assumption is then that the superposition principle applies, that is, the effects of two different stress increments on the time-dependent strain can be superposed. Under service stress levels this is a reasonable assumption.

Visco-elasticity theory uses hereditary integrals. This has distinct advantages when constructing analytical solutions, since then the Laplace transform technique can be used to reduce the time-dependent problem to an ordinary linear-elastic problem, for which a solution may exist. After the elastic solution has been found a backtransformation is carried out to obtain the stress and strain evolution in the time-domain.

For numerical applications, hereditary integrals are not so easily handled. In a straightforward implementation they require storage of the entire stress or strain history. Since this must be done for each integration point, large-scale two and three-dimensional applications are effectively excluded in this approach. For this reason the kernel of the hereditary integral is normally expanded in a series, and only the first five to seven terms are retained. In this strategy the stress or strain history is memorised via a limited, constant number of internal variables (Zienkiewicz et al. 1968, Taylor et al. 1970, Bazant and Wu 1973, 1974).

Creep and Shrinkage of Concrete. Edited by Z.P. Bažant and I. Carol. © RILEM.
Published by E & FN Spon, 2–6 Boundary Row, London SE1 8HN. ISBN 0 419 18630 1.

In this paper we shall review numerical approaches to visco-elasticity which set out to describe concrete creep behaviour. Both 'long-term' creep behaviour and creep at early ages are considered. Next, the visco-elastic creep models will be combined with smeared-crack models. A numerical example that involves cracking in an axisymmetric early-age concrete structure is presented to demonstrate the possibilities of such approaches. The discussion is continued with an investigation into well-posedness of the rate boundary value problem in the presence of cracking. It will be investigated to which extent the stabilizing influence of viscosity, which has been proven for high loading rates, also holds for slow processes, that is when inertia effects are absent. A final important aspect when carrying out time-dependent calculations is the magnitude of the time step. An automatic time stepping procedure will be derived which is inspired by the well-known path-following solution procedures commonly adopted in static analyses.

2 Concrete creep and large-scale computations

As point of departure we shall utilise the creep formulation

$$\boldsymbol{\varepsilon}(t) = \int_0^t J(t,\tau)\,\mathbf{C}\,\dot{\boldsymbol{\sigma}}(\tau)\,\mathrm{d}\tau\,. \tag{1}$$

In eq. (1), $\dot{\boldsymbol{\sigma}}$ is the stress rate tensor, $J(t,\tau)$ is the creep function, and the components of $\mathbf{C}$ are defined by

$$C_{ijkl} = \tfrac{1}{2}(1+\nu)[\delta_{ik}\delta_{jl} + \delta_{il}\delta_{jk}] - \nu\,\delta_{ij}\delta_{kl}\,, \tag{2}$$

with ν Poisson's ratio, which is assumed to be independent of the time of load application $\tau = t$ and δ_{ij} the Kronecker delta. Following common practice (*cf.* Bazant *et al.* 1988) we now separate the creep function into an age-dependent Young's modulus $E(\tau)$ which represents the instantaneous elastic stiffness, and a function $J_c(t,\tau)$ which purely reflects time-dependent effects:

$$J(t,\tau) = \frac{1}{E(\tau)} + J_c(t,\tau)\,. \tag{3}$$

This identity is substituted into the creep formulation (1) to yield:

$$\boldsymbol{\varepsilon}(t) = \int_0^t [E^{-1}(\tau) + J_c(t,\tau)]\,\mathbf{C}\,\dot{\boldsymbol{\sigma}}(\tau)\,\mathrm{d}\tau\,. \tag{4}$$

We now differentiate eq. (4) and use Leibniz' rule to obtain

$$\dot{\boldsymbol{\varepsilon}}(t) = E^{-1}(t)\mathbf{C}\,\dot{\boldsymbol{\sigma}}(t) + \int_0^t J'(t,\tau)\,\mathbf{C}\,\dot{\boldsymbol{\sigma}}(\tau)\,\mathrm{d}\tau\,. \tag{5}$$

with $J'(t,\tau)$ the first derivative of J_c (or equivalently J) with respect to t.

The use of constitutive relations in displacement-method based finite elements is greatly facilitated if the stress rate is explicitly written as a function of the strain rate and the strain or stress history. For this reason (5) is rearranged as

$$\dot{\boldsymbol{\sigma}}(t) = E(t)\left[\mathbf{D}\,\dot{\boldsymbol{\varepsilon}}(t) - \int_0^t J'(t,\tau)\,\dot{\boldsymbol{\sigma}}(\tau)\,\mathrm{d}\tau\right], \tag{6}$$

with $\mathbf{D} = \mathbf{C}^{-1}$. Setting

$$\Delta t = t_{i+1} - t_i \tag{7}$$

$$\Delta\boldsymbol{\sigma} = \boldsymbol{\sigma}(t_{i+1}) - \boldsymbol{\sigma}(t_i) \tag{8}$$

$$\Delta\boldsymbol{\varepsilon} = \boldsymbol{\varepsilon}(t_{i+1}) - \boldsymbol{\varepsilon}(t_i)\,, \tag{9}$$

we can integrate eq. (6) to give

$$\Delta\boldsymbol{\sigma} = \int_{t=t_i}^{t_{i+1}} E(t)\,\mathbf{D}\,\dot{\boldsymbol{\varepsilon}}\,\mathrm{d}t - \int_{t=t_i}^{t_{i+1}} E(t) \int_{\tau=0}^{t} J'(t,\tau)\,\dot{\boldsymbol{\sigma}}(\tau)\,\mathrm{d}\tau\,\mathrm{d}t \tag{10}$$

which can be approximated by the finite sum

$$\Delta\boldsymbol{\sigma} = E(t^*)\,\mathbf{D}\,\Delta\boldsymbol{\varepsilon} - \sum_{q=0}^{n-1} E(t^*)\,J'(t^*,\tau_q)\,\Delta\boldsymbol{\sigma}_q\,\Delta t_q\,. \tag{11}$$

with $t_i \le t^* \le t_{i+1}$. According to (11) the stress increment is computed from the strain increment $\Delta\boldsymbol{\varepsilon}$ of the current time step and the stress increments $\Delta\boldsymbol{\sigma}_q$ of all previous time steps. The product of an additional strain increment $\Delta\boldsymbol{\varepsilon}$ and the actual Young's modulus $E(t)$ increases the current stress, while the second term in eq. (11) describes the relaxation process. The disadvantages of such an algorithm are the fact that the entire load history of each material point needs to be stored and that the computational times explode as the period increases which has to be analysed. Even for modern computer equipment this is an impossible requirement for realistic (three-dimensional) engineering structures.

To obviate the above disadvantage most finite element programs use an algorithm that is based on an expansion of the kernel $J(t,\tau)$ of the hereditary integral. Commonly, negative exponential powers (Dirichlet series) of polynomials (Taylor series) are used for this purpose. The first approach is usually adopted for long-term creep simulations, the period of consideration stretching over years to several decades. The other procedure can be advantageously adopted for short-term creep processes, e.g., in early-age concrete.

2.1 Long-term processes: Dirichlet series

An alternative approach to expanding the creep function $J(t,\tau)$ into a series of negative exponential powers would be to express the stress $\boldsymbol{\sigma}$ directly as a functional of the strain history:

$$\boldsymbol{\sigma}(t) = \int_0^t R(t,\tau)\,\mathbf{D}\,\dot{\boldsymbol{\varepsilon}}(\tau)\,\mathrm{d}\tau\,, \tag{12}$$

and then to expand the relaxation function R in a series of negative exponential powers:

$$R(t,\tau)=E_0(\tau)+\sum_{\alpha=1}^{N}E_\alpha(\tau)\exp(-(t-\tau)/\lambda_\alpha)) \,. \tag{13}$$

with λ_α the relaxation times of the individual chain elements. Mechanically, the model that results can be interpreted as a Maxwell chain model (Bazant and Wu 1974). The resulting algorithm reads:

$$\Delta\boldsymbol{\sigma}=E_0(t^*)\mathbf{D}\Delta\boldsymbol{\varepsilon}+\sum_{\alpha=1}^{N}[1-\exp(-\Delta t/\lambda_\alpha)]\left[\frac{E_\alpha(t^*)}{\Delta t/\lambda_\alpha}\mathbf{D}\Delta\boldsymbol{\varepsilon}-\boldsymbol{\sigma}_\alpha(t_i)\right]. \tag{14}$$

The merits and disadvantages of either starting from a creep function or from a relaxation function have been discussed extensively in the literature (e.g., Bazant *et al.* 1988). They primarily become manifest in case of aging solids, so that the spring moduli E_α are not constant in time. However, for the numerical implementation it does not seem to matter which point of departure is chosen (Anderson *et al.* 1988).

The accuracy of the above integration scheme hinges on the assumption that $\dot{\boldsymbol{\varepsilon}}$ and E_α do not vary much during the time step. Indeed, eq. (14) is exact if $\dot{\boldsymbol{\varepsilon}}$ and E_α are constant during the time step. For a non-aging solid the assumption that E_α remains constant during a time step is satisfied rigorously, but even for an aging solid E_α usually varies so slowly with time that it mostly entails no serious errors. In the absence of cracks, the assumption that $\dot{\boldsymbol{\varepsilon}}$ also remains constant, is usually reasonable. When we have crack initiation or propagation, the assumption is more questionable. As we will show hereafter, $\dot{\boldsymbol{\varepsilon}}$ must then be replaced by $\dot{\boldsymbol{\varepsilon}}^{co}$, the part of the total strain rate that applies to the concrete. Since $\dot{\boldsymbol{\varepsilon}}^{cr}$ can vary quite abruptly over a time step, $\dot{\boldsymbol{\varepsilon}}^{co}$ may also show considerable changes. This implies that time steps must be chosen much smaller when cracks are present than when they are absent.

2.2 Short-term processes: Taylor series

For creep in early-age concrete only relatively short time spans have to be analysed. On the other hand, the stress fluctuations during this period may be more pronounced than in 'long-term' processes. For this reason it may be advantageous to develop $J(t,\tau)$ in a Taylor series instead of in a Dirichlet series. We consider the class of creep functions for which

$$J(t,\tau)=f(\tau)\cdot g(t-\tau) \,, \tag{15}$$

which is sufficiently broad to encompass most commonly used creep models. For instance the power law

$$J(t,\tau)=\frac{1}{E(\tau)}(1+a\,\tau^{-d}(t-\tau)^p) \,, \tag{16}$$

with a, d and p material parameters, falls in this category. We now expand $J'(t,\tau)$ in a Taylor series around $\tau=t_d$. This gives:

$$J'(t,\tau)=\sum_{\alpha=0}^{N} f(\tau)h_\alpha(t-t_d)\tau^\alpha\,, \tag{17}$$

which is convergent for $0<t\le 2t_d$. Substitution in eq. (10) and separating the integration domain into a part from $\tau=0$ to t_i and a part from $\tau=t_i$ to t yields

$$\Delta\boldsymbol{\sigma}=\int_{t=t_i}^{t_{i+1}} E(t)\,\mathbf{D}\,\dot{\boldsymbol{\varepsilon}}\,\mathrm{d}t-\sum_{\alpha=0}^{N}\left[\int_{t=t_i}^{t_{i+1}} E(t)\int_{\tau=0}^{t_i} f(\tau)h_\alpha(t-t_d)\tau^\alpha\dot{\boldsymbol{\sigma}}(\tau)\,\mathrm{d}\tau\,\mathrm{d}t + \int_{t=t_i}^{t_{i+1}} E(t)\int_{\tau=t_i}^{t} f(\tau)h_\alpha(t-t_d)\tau^\alpha\dot{\boldsymbol{\sigma}}(\tau)\,\mathrm{d}\tau\,\mathrm{d}t\right]. \tag{18}$$

Separating the integrals of the first expression between brackets and exchanging the order of integration in the second term leads to

$$\Delta\boldsymbol{\sigma}=\int_{t=t_i}^{t_{i+1}} E(t)\,\mathbf{D}\,\dot{\boldsymbol{\varepsilon}}\,\mathrm{d}t-\sum_{\alpha=0}^{N}\left[\int_{t=t_i}^{t_{i+1}} E(t)\,h_\alpha(t-t_d)\,\mathrm{d}t\int_{\tau=0}^{t_i} f(\tau)\tau^\alpha\dot{\boldsymbol{\sigma}}(\tau)\,\mathrm{d}\tau + \int_{t=\tau}^{t_{i+1}}\int_{\tau=t_i}^{t_{i+1}} E(t)\,h_\alpha(t-t_d)f(\tau)\tau^\alpha\dot{\boldsymbol{\sigma}}(\tau)\,\mathrm{d}\tau\,\mathrm{d}t\right]. \tag{19}$$

The integration between t_i and t_{i+1} is now carried out by a generalised mid-point rule, so that the integrals are evaluated for $t=t^*$. In the example that is presented in the next section $t^*=(t_i+t_{i+1})/2$ has been used. This numerical integration rule has also been applied to the integration from $t=\tau$ to t_{i+1}. Assuming a constant stress rate during the time step, $\dot{\boldsymbol{\sigma}}=\Delta\boldsymbol{\sigma}/\Delta t$, we obtain

$$\Delta\boldsymbol{\sigma}=E(t^*)[\mathbf{D}\Delta\boldsymbol{\varepsilon}-\Delta t\sum_{\alpha=0}^{N}A_\alpha h_\alpha(t^*-t_d)]-\frac{1}{2}\Delta t\sum_{\alpha=0}^{N}(t^*)^\alpha f(t^*)h_\alpha(t^*-t_d)\Delta\boldsymbol{\sigma}\,, \tag{20}$$

with

$$A_\alpha=\sum_{j=1}^{i} t_j^\alpha f(t_j)\Delta\boldsymbol{\sigma}_j \tag{21}$$

The final expression for $\Delta\boldsymbol{\sigma}$ is now given by:

$$\Delta\boldsymbol{\sigma}=\frac{E(t^*)[\mathbf{D}\Delta\boldsymbol{\varepsilon}-\sum_{\alpha=0}^{N}A_\alpha h_\alpha(t^*-t_d)\Delta t]}{1+\frac{1}{2}\Delta t\sum_{\alpha=0}^{N}(t^*)^\alpha f(t^*)h_\alpha(t^*-t_d)}\,. \tag{22}$$

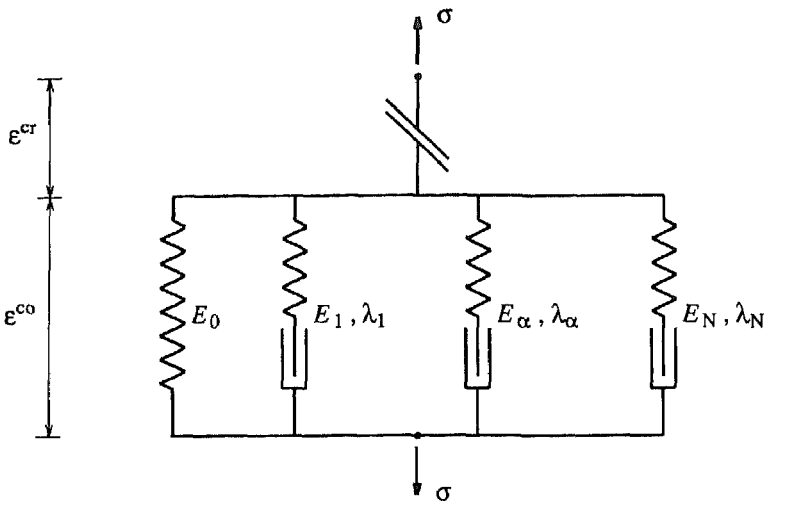

Figure 1. Maxwell chain model coupled in series with a smeared-crack model.

3 Visco-elasticity and fracture models

3.1 Smeared crack modelling

The above derivations do not take into account the possibility of cracking. However, such an extension can be incorporated straightforwardly if a smeared crack model is used that assumes a decomposition of the strain tensor into a concrete strain $\boldsymbol{\varepsilon}^{co}$ and a crack strain $\boldsymbol{\varepsilon}^{cr}$. Then, the only modification that has to be made is the replacement of the total strain increment $\Delta\boldsymbol{\varepsilon}$ by the concrete strain increment $\Delta\boldsymbol{\varepsilon}^{co}$ in the algorithmic expressions that compute the stress increment $\Delta\boldsymbol{\sigma}$ from the strain increment and the stress or strain history. For instance, when a Maxwell chain model is used for the concrete part [*cf.* eq. (14)] the following incremental relation between stress increment and concrete strain increment results:

$$\Delta\boldsymbol{\sigma}=E_0(t^*)\mathbf{D}\Delta\boldsymbol{\varepsilon}^{co}+\sum_{\alpha=1}^{N}[1-\exp(-\Delta t/\lambda_\alpha)]\left[\frac{E_\alpha(t^*)}{\Delta t/\lambda_\alpha}\mathbf{D}\Delta\boldsymbol{\varepsilon}^{co}-\boldsymbol{\sigma}_\alpha(t_i)\right], \tag{23}$$

see also the graphical representation in Figure 1. For future use it is convenient to replace this identity by the expression

$$\Delta\boldsymbol{\sigma}=\mathbf{D}^{co}\Delta\boldsymbol{\varepsilon}^{co}+\tilde{\boldsymbol{\sigma}} \tag{24}$$

with

$$\mathbf{D}^{co}=E_0(t^*)\mathbf{D}+\sum_{\alpha=1}^{N}[1-\exp(-\Delta t/\lambda_\alpha)]\frac{E_\alpha(t^*)}{\Delta t/\lambda_\alpha}\mathbf{D} \tag{25}$$

the instantaneous stiffness matrix of the concrete and

$$\tilde{\boldsymbol{\sigma}} = -\sum_{\alpha=1}^{N} [1 - \exp(-\Delta t/\lambda_\alpha)]\boldsymbol{\sigma}_\alpha(t_i) \tag{26}$$

the relaxation term.

The additive decomposition of the total strain into a concrete part $\boldsymbol{\varepsilon}^{co}$ and a cracking part $\boldsymbol{\varepsilon}^{cr}$ reads in an incremental form (de Borst and Nauta 1985, de Borst 1987, Rots 1988):

$$\Delta\boldsymbol{\varepsilon} = \Delta\boldsymbol{\varepsilon}^{co} + \Delta\boldsymbol{\varepsilon}^{cr} . \tag{27}$$

As pointed out by de Borst and Nauta (1985) and de Borst (1987) the crack strain increment $\Delta\boldsymbol{\varepsilon}^{cr}$ can again be composed of several contributions:

$$\Delta\boldsymbol{\varepsilon}^{cr} = \Delta\boldsymbol{\varepsilon}_1^{cr} + \Delta\boldsymbol{\varepsilon}_2^{cr} + ... \tag{28}$$

where $\Delta\boldsymbol{\varepsilon}_1^{cr}$ is the strain increment owing to a primary crack, $\Delta\boldsymbol{\varepsilon}_2^{cr}$ is the strain increment owing to a secondary crack and so on. For simplicity sake this enhancement will not be pursued here.

The relation between the crack strain increment of a particular crack (either primary or secondary) and the stress increment is conveniently defined in the coordinate system which is aligned with the crack. This necessitates a transformation between the crack strain increment $\Delta\boldsymbol{\varepsilon}^{cr}$ of crack n in the global x,y-coordinate system and a crack strain increment $\Delta\mathbf{e}^{cr}$ which is expressed in local n,t-coordinates. Restricting the treatment to a two-dimensional configuration (which is not essential), we observe that a crack only has a normal strain increment Δe^{cr} (mode-I) and a shear strain increment $\Delta\gamma^{cr}$ (mode-II), so that

$$\Delta\mathbf{e}^{cr} = [\Delta e^{cr}, \Delta\gamma^{cr}]^T . \tag{29}$$

The relation between $\Delta\boldsymbol{\varepsilon}^{cr}$ and $\Delta\mathbf{e}^{cr}$ reads

$$\Delta\boldsymbol{\varepsilon}^{cr} = \mathbf{N}\Delta\mathbf{e}^{cr} , \tag{30}$$

with

$$\mathbf{N} = \begin{bmatrix} \cos^2\theta & -\sin\theta\cos\theta \\ \sin^2\theta & \sin\theta\cos\theta \\ 2\sin\theta\cos\theta & \cos^2\theta - \sin^2\theta \end{bmatrix} , \tag{31}$$

and θ the inclination angle of the normal of the crack with the x-axis. In a similar way, we can define a vector $\Delta\mathbf{s}$

$$\Delta\mathbf{s} = [\Delta s , \Delta t]^T , \tag{32}$$

with Δs the normal and Δt the shear stress increment in the crack coordinate system. The relation between the stress increment in the global coordinate system $\Delta\boldsymbol{\sigma}$ and the stress increment vector $\Delta\mathbf{s}$ reads

$$\Delta \mathbf{s} = \mathbf{N}^T \Delta \boldsymbol{\sigma} \,. \tag{33}$$

To complete the system of equations, we use the general form of the integrated evolution equations for visco-elasticity (24) as constitutive relation for the concrete and a stress-strain relation for the smeared cracks which we assume to have the following format:

$$\Delta \mathbf{s} = \mathbf{D}^{cr} \Delta \mathbf{e}^{cr} + \boldsymbol{\Lambda} \,, \tag{34}$$

with $\mathbf{D}^{cr}$ a 2×2 matrix and $\boldsymbol{\Lambda}$ a vector that contains the viscous or rate effects in the cracks. In dynamic fracture analyses of concrete inclusion of the latter term proved necessary to restore well-posedness of the initial value problem (Sluys 1992). A discussion for quasi-static loading conditions is given below.

Using eqs. (24)-(34) we can develop the tangential stiffness relation for the cracked concrete:

$$\Delta \boldsymbol{\sigma} = \left[\mathbf{I} - \mathbf{D}^{co} \mathbf{N} [\mathbf{D}^{cr} + \mathbf{N}^T \mathbf{D}^{co} \mathbf{N}]^{-1} \mathbf{N}^T \right] (\mathbf{D}^{co} \Delta \boldsymbol{\varepsilon} + \tilde{\boldsymbol{\sigma}}) + \mathbf{D}^{co} \mathbf{N} [\mathbf{D}^{cr} + \mathbf{N}^T \mathbf{D}^{co} \mathbf{N}]^{-1} \boldsymbol{\Lambda} \,. \tag{35}$$

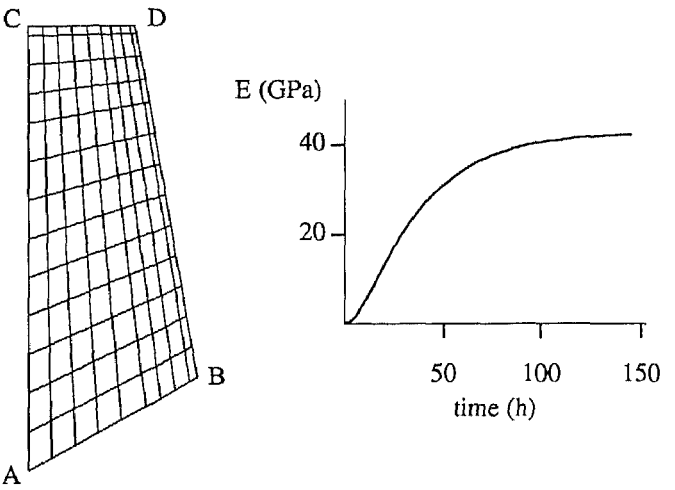

Figure 2. Discretisation of one leg of tetrapod structure (left) and evolution of Young's modulus at point A (right).

3.2 A case study: cracking in early-age concrete

An example is now presented. It involves the calculation of the stresses during the hardening process in early-age concrete. The structure that has been considered is a tetrapod, which is used as a cover element for a breakwater. The full structure has four axisymmetric legs. In the analyses described here only one leg has been modelled and it has been assumed that full axisymmetry could be adopted, including the boundary AB. This is a simplification, since the connection with the other legs of the tetrapod can never be axisymmetric. The element mesh for the stress calculation of one leg is shown

in Figure 2. In line with the assumption of full axisymmetry smooth boundary conditions have been imposed along AB and AC.

The problem of stress evolution in early-age concrete is essentially a coupled thermo-mechanical problem. However, the coupling is rather weak and the thermal and stress analyses have been carried out separately, the result of the thermal finite element analysis being the input for the stress analysis. Other input data for the stress analysis that result from the thermal analysis are the degree of maturity as a function of time and the evolution of Young's modulus. The particular expressions that have been used in the thermal analysis for the rate of heat production, the thermal conductivity and the heat capacity can be found in Reinhardt *et al.* (1982) and de Borst (1989). Van den Bogert *et al.* (1987) and de Borst (1989) list the expressions that have been used for the evolution of the degree of maturity and the Young's modulus. As an example the growth of the Young's modulus in point A is given in the right part of Figure 2.

In the stress analysis the power law of eq. (16) has been employed with the parameters $a=4.518$, $d=0.35$, $p=0.3$ and a development time $t_d=0.3024\cdot10^6$ s. The linear coefficient of thermal expansion was $0.011\cdot10^{-3}$ m/mK. Poisson's ratio was taken equal to 0.2. Shrinkage caused by drying of the hardening cement paste has not been taken into account, neither were rate effects considered for the smeared-crack model ($\Lambda=0$). Tension-softening was included in the smeared crack model with a tensile strength $f_t=2$ MPa and a linear softening branch with an ultimate strain $\varepsilon_u=0.033$ at which the tensile capacity is exhausted.

For the stress analysis eight-noded isoparametric elements were used with a 3×3 Gaussian integration. The finite element calculations were carried out in 31 time steps, starting with increments of 1 h up to 10 h for the last ten steps. A Modified Newton-Raphson procedure was used to achieve equilibrium within each time step. The convergence criterion was based on the Euclidean norm of the incremental displacements and was set equal to 10^{-6}. Normally, 8-12 iterations were needed to comply with this requirement, although after extensive cracking the requirement could not be satisfied within the allotted number of iterations (20).

The crack patterns that result from the finite element simulations are shown in Figure 3 for $t=50$ h and $t=70$ h, and in Figure 4 for $t=100$ h and $t=150$ h. Note that the little rectangles that appear in Figure 4 and $t=150$ h represent cracking due to tensile hoop stresses. The centre pictures always represent the standard case with a tensile strength $f_t=2$ MPa and a diameter of the leg of the tetrapod $D=2$ m. The right pictures are for the same structural size, but for a lower tensile strength ($f_t=1.5$ MPa), while the left pictures show the crack evolution for the same tensile strength, but for a smaller diameter ($D=1.5$ m). We clearly observe the faster spreading of the cracking for the larger diameter and for the smaller tensile strength. Also the zones in which cracks propagate are different as can be observed clearly at $t=70$ h for the variation in tensile strength. Of course, a more realistic analysis should include a tensile strength that is a function of the time (Brameshuber and Hilsdorf 1989).

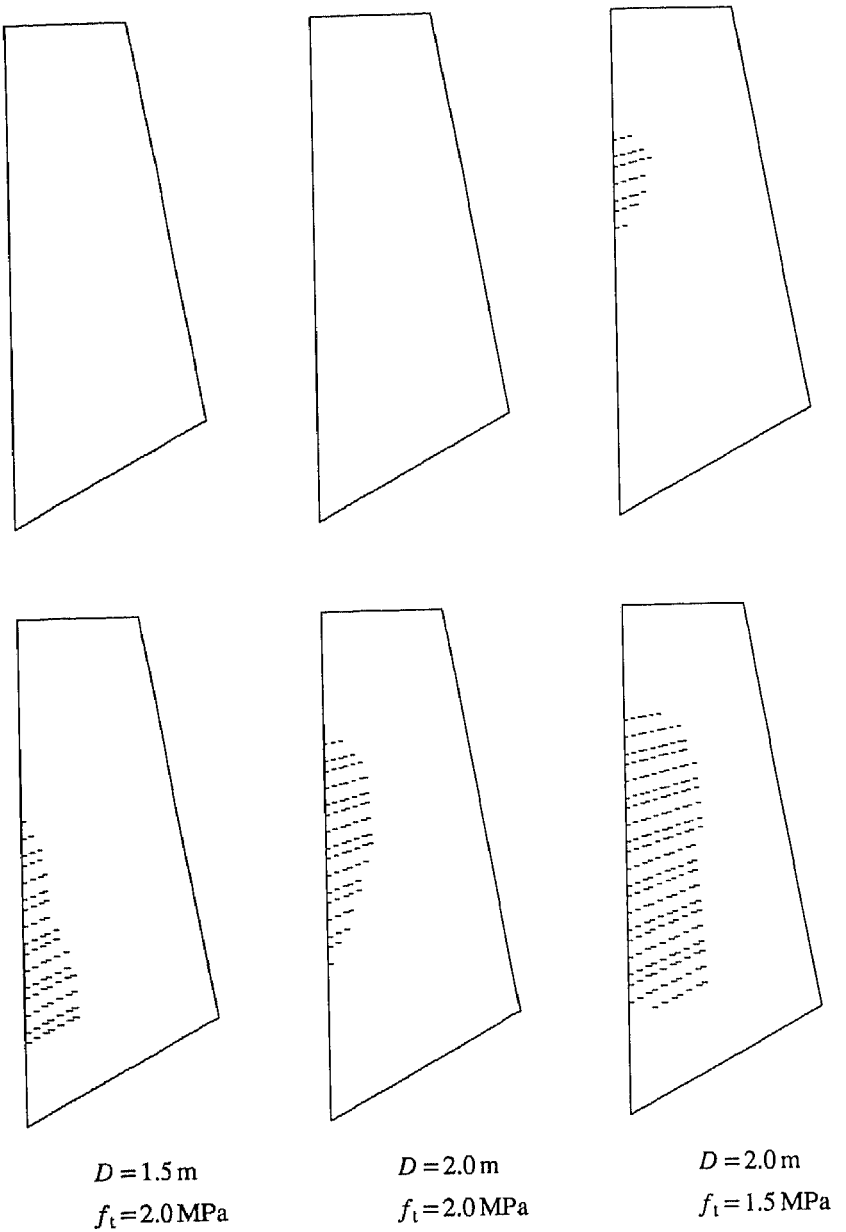

Figure 3. Crack patterns for $t = 50$ h (top) and $t = 70$ h (bottom).

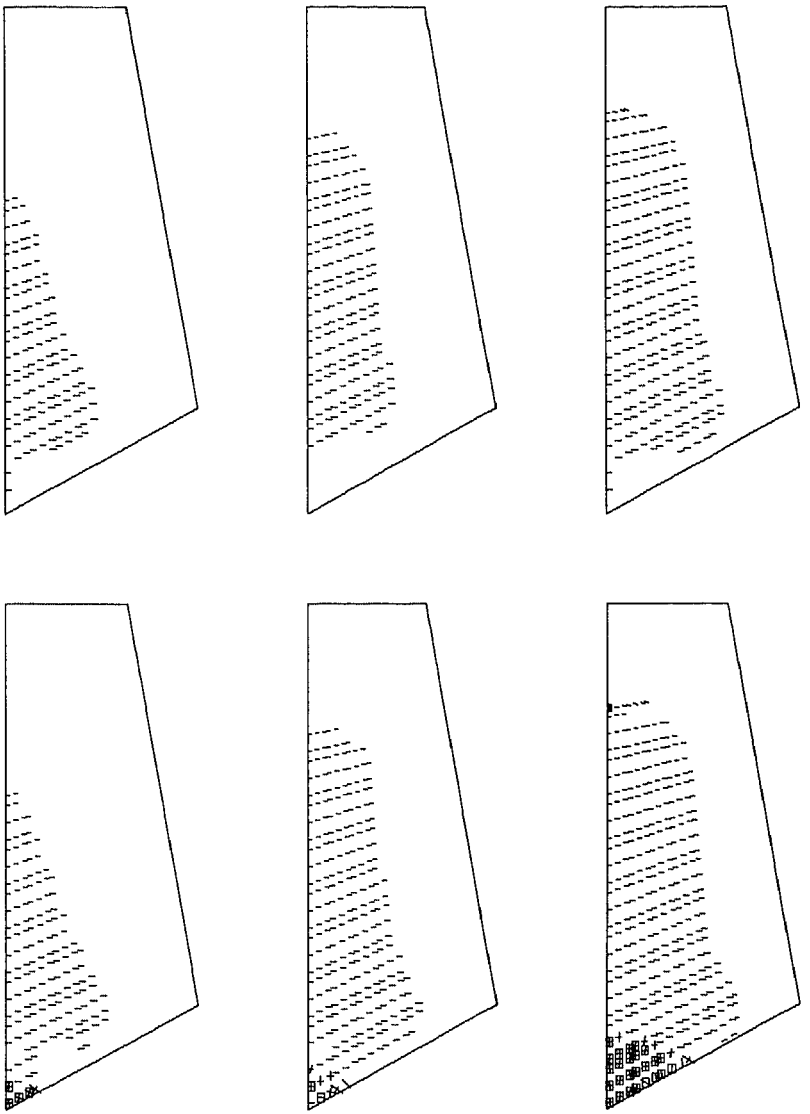

$D = 1.5$ m
$f_t = 2.0$ MPa

$D = 2.0$ m
$f_t = 2.0$ MPa

$D = 2.0$ m
$f_t = 1.5$ MPa

Figure 4. Crack patterns for $t = 100$ h (top) and $t = 150$ h (bottom).

4 Well-posedness of the rate boundary value problem

The model embodied in eq. (35) contains viscous contributions to the concrete strain $\Delta\boldsymbol{\varepsilon}^{co}$ (eqs. (24)-(26)) and to the local crack strain $\Delta\mathbf{e}^{cr}$ (34). Especially the latter contribution is important and has a stabilising influence on the creep-fracture process. In a classical treatment of fracture the formation of cracks is a discontinuous process in space and time. A local jump-wise solution for the strains develops instantaneously in time. This problem is usually referred to as loss of ellipticity in quasi-static problems and loss of hyperbolicity in dynamic problems (Hill 1962, Rice 1976). Computational modelling of smeared crack constitutive relations which do not incorporate a characteristic length or time scale then leads to mesh-dependent results.

The contribution of viscosity to the concrete strain has only a slight effect on the fracture process and does not change the character of the equations, i.e. it does not prevent loss of ellipticity or hyperbolicity, respectively. On the other hand, the addition of a viscous component to the crack stress affects the fracture process and prevents the initial value problem from becoming elliptic (Sluys 1992). The regularising influence of viscosity in the rate boundary value problem will be discussed here. Because the viscosity contribution to the concrete plays a minor role its influence will not be considered.

If we consider a direction normal to the crack plane and depart from eq. (34) we have

$$\Delta s = h\,\Delta e^{cr} + m\,\frac{\partial \Delta e^{cr}}{\partial t}\,, \tag{36}$$

with h the mode-I component of $\mathbf{D}^{cr}$ and $m\,\partial\Delta e^{cr}/\partial t$ the mode-I component of $\boldsymbol{\Lambda}$. The parameter m represents the viscosity of the cracked material. Note that t denotes time and not a direction aligned with the crack. If we substitute $\Delta e^{cr} = \Delta e - \Delta e^{e}$ and $\Delta e^{e} = \Delta s/E$ into eq. (36) we obtain

$$(h+E)\Delta s + m\,\frac{\partial \Delta s}{\partial t} = h\,E\,\Delta e + m\,E\,\frac{\partial \Delta e}{\partial t}\,. \tag{37}$$

Substitution of the kinematic equation $\Delta e = \partial \Delta u/\partial n$ into eq. (37), with u the displacement in the n-direction normal to the crack, and differentiation with respect to n yields

$$\frac{\partial}{\partial n}\left((h+E)\Delta s + m\,\frac{\partial \Delta s}{\partial t}\right) = h\,E\,\frac{\partial^2 \Delta u}{\partial n^2} + m\,E\,\frac{\partial^3 \Delta u}{\partial n^2 \partial t}\,. \tag{38}$$

Assuming equilibrium over the time step, i.e. $\partial\Delta s/\partial n = 0$, the left hand side of eq. (38) becomes zero and the viscous fracture process is described by the right hand side of this equation. To investigate solutions in the n–t plane the characteristic determinant of the following system is determined:

$$\begin{bmatrix} 0 & m & 0 \\ \mathrm{d}t & \mathrm{d}n & 0 \\ 0 & \mathrm{d}t & \mathrm{d}n \end{bmatrix} \begin{bmatrix} \dfrac{\partial^3 \Delta u}{\partial n \partial^2 t} \\ \dfrac{\partial^3 \Delta u}{\partial^2 n \partial t} \\ \dfrac{\partial^3 \Delta u}{\partial^3 n} \end{bmatrix} = \begin{bmatrix} -h \dfrac{\partial^2 \Delta u}{\partial n^2} \\ \mathrm{d}\left(\dfrac{\partial^2 \Delta u}{\partial n \partial t}\right) \\ \mathrm{d}\left(\dfrac{\partial^2 \Delta u}{\partial^2 n}\right) \end{bmatrix}. \tag{39}$$

With the determinant equal to zero the characteristic directions $\mathrm{d}n/\mathrm{d}t = 0$. This means that the rate boundary value problem does not become hyperbolic but is of the parabolic type. Consequently, the problem remains well-posed and no mathematical or numerical problems are to be expected. A characteristic length and time scale are present in the model, which prevent the occurrence of a jump-wise solution and remove the mesh-dependence in the finite element analysis. However, it is noted that if the creep-fracture process evolves to a steady state situation the third-order derivative term in eq. (38) no longer dominates the second-order term (or the viscosity m should be taken artificially high). The derivation of the characteristic directions no longer holds and ellipticity of the rate boundary value problem is lost in the limit.

5 An automatic time-stepping procedure

In finite element analyses a time-marching procedure is normally employed to trace the evolution of stresses and strains and to monitor crack propagation. Especially during rapid crack extension a small time step is needed in order that a converged solution can be obtained in the iterative equilibrium-finding procedure. In purely static analyses arc-length, or path-following procedures, have gained much popularity to adapt the magnitude of the load increment in an automatic fashion (Riks 1979, Ramm 1981, Crisfield 1981). Below we shall demonstrate how this methodology can be extended to quasi-static processes where the time plays a role, so that the time step is changed automatically when the degree of non-linearity of the process varies.

When an arc-length method is applied in the time domain, the time increment Δt does not remain constant from iteration i to iteration $i+1$, but changes from Δt_i to Δt_{i+1}. The iterative change is denoted by the δ-symbol

$$\delta t_{i+1} = \Delta t_{i+1} - \Delta t_i \tag{40}$$

similar to the iterative change in the displacement vector:

$$\delta \mathbf{u}_{i+1} = \Delta \mathbf{u}_{i+1} - \Delta \mathbf{u}_i \,. \tag{41}$$

When $\mathbf{B}$ is the matrix that connects the nodal displacements to the strains in the integration points of the finite elements and if we assemble all external actions at time t_{i+1} in a vector $\mathbf{r}_{i+1}$, then equilibrium of the discretised system reads:

$$\int_V \mathbf{B}^{\mathrm{T}} \boldsymbol{\sigma}_{i+1} \mathrm{d}V = \mathbf{r}_{i+1} \,. \tag{42}$$

Introduction of the normalised load vector $\mathbf{r}$ and the current load factor λ_{i+1} at iteration $i+1$, such that $\mathbf{r}_{i+1} = \lambda_{i+1}\,\mathbf{r}$, permits rewriting of (42) as

$$\int_V \mathbf{B}^T \boldsymbol{\sigma}_{i+1} dV = \lambda_{i+1} \mathbf{r} . \tag{43}$$

We now expand the stress and the load factor at the end of iteration $i+1$ in a truncated Taylor series:

$$\boldsymbol{\sigma}_{i+1} = \boldsymbol{\sigma}_i + \mathbf{D}_i \mathbf{B} \delta \mathbf{u}_{i+1} + \dot{\boldsymbol{\sigma}}_i \delta t_{i+1} \tag{44}$$

with $\mathbf{D}_i$ the tangential stress-strain relation at the end of iteration i and

$$\lambda_{i+1} = \lambda_i + \dot{\lambda}_i \delta t_{i+1} \tag{45}$$

When, for instance a Maxwell chain is used, $\mathbf{D}_i$ and $\dot{\boldsymbol{\sigma}}_i$ are found by differentiating the secant relation (14) with respect to the strain and the time, respectively, as follows

$$\mathbf{D}_i = E_0(t^*)\mathbf{D} + \sum_{\alpha=1}^{N} [1 - \exp(-\Delta t/\lambda_\alpha)] \frac{E_\alpha(t^*)}{\Delta t/\lambda_\alpha} \mathbf{D} . \tag{46}$$

and

$$\dot{\boldsymbol{\sigma}}_i = \sum_{\alpha=1}^{N} \frac{1}{\lambda_\alpha} \exp(-\Delta t/\lambda_\alpha) \left[\frac{E_\alpha(t^*)}{\Delta t/\lambda_\alpha} \mathbf{D} \Delta \boldsymbol{\varepsilon} - \boldsymbol{\sigma}_\alpha(t_i) \right]$$

$$- \sum_{\alpha=1}^{N} [1 - \exp(-\Delta t/\lambda_\alpha)] \frac{E_\alpha(t^*)}{\Delta t^2/\lambda_\alpha} \mathbf{D} \Delta \boldsymbol{\varepsilon} . \tag{47}$$

The next step is to substitute eqs. (44) and (45) in eq. (43). The result is

$$\mathbf{K}_i \delta \mathbf{u}_{i+1} = \lambda_i \mathbf{r} - \int_V \mathbf{B}^T \boldsymbol{\sigma}_i dV + \delta t_{i+1} [\dot{\lambda}_i \mathbf{r} - \int_V \mathbf{B}^T \dot{\boldsymbol{\sigma}}_i dV] . \tag{48}$$

with the tangent stiffness matrix conventionally defined as

$$\mathbf{K}_i = \int_V \mathbf{B}^T \mathbf{D}_i \mathbf{B} dV . \tag{49}$$

Defining $\mathbf{p}_i$ and $\mathbf{q}_i$ as

$$\mathbf{p}_i = \lambda_i \mathbf{r} - \int_V \mathbf{B}^T \boldsymbol{\sigma}_i dV + \Delta t_i [\dot{\lambda}_i \mathbf{r} - \int_V \mathbf{B}^T \dot{\boldsymbol{\sigma}}_i dV] \tag{50}$$

and

$$\mathbf{q}_i = \dot{\lambda}_i \mathbf{r} - \int_V \mathbf{B}^T \dot{\boldsymbol{\sigma}}_i dV , \tag{51}$$

respectively, we can rewrite eq. (48) as

$$\mathbf{K}_i \delta \mathbf{u}_{i+1} = \mathbf{p}_i + \Delta t_{i+1} \mathbf{q}_i . \tag{52}$$

Furthermore, we define

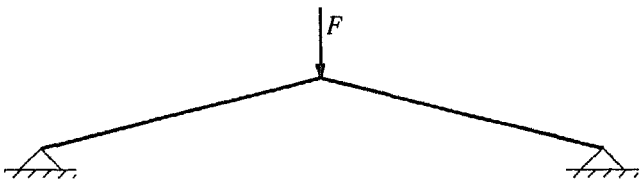

Figure 5. Simple truss model used for assessment of automatic time-stepping procedure.

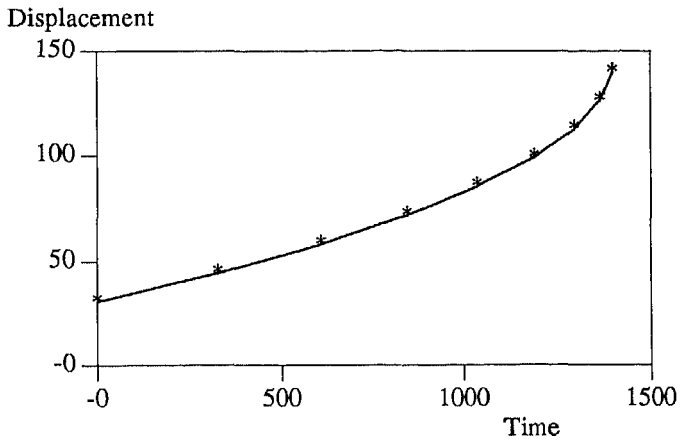

Figure 6. Time-displacement diagram for simple truss structure of Figure 5.

$$\delta \mathbf{u}_{i+1}^{\mathrm{I}} = \mathbf{K}_i^{-1}\, \mathbf{p}_i \tag{53}$$

and

$$\delta \mathbf{u}_{i+1}^{\mathrm{II}} = \mathbf{K}_i^{-1}\, \mathbf{q}_i \tag{54}$$

After computing $\mathbf{u}_{i+1}^{\mathrm{I}}$ and $\mathbf{u}_{i+1}^{\mathrm{II}}$ the variable time step Δt_{i+1} can be calculated from a constraint condition that the incremental displacements remain constant over the time measured in some norm. For instance, the L_2-norm in the n-dimensional displacement space has gained much popularity (Crisfield 1981). In its linearised version it reads (Ramm 1981):

$$\Delta \mathbf{u}_i^{\mathrm{T}} \delta \mathbf{u}_{i+1}^{\mathrm{I}} = 0\,. \tag{55}$$

Substitution of (53) and (54) in (55) then yields

$$\Delta t_{i+1} = -\frac{\Delta \mathbf{u}_i^{\mathrm{T}} \delta \mathbf{u}_{i+1}^{\mathrm{I}}}{\Delta \mathbf{u}_i^{\mathrm{T}} \delta \mathbf{u}_{i+1}^{\mathrm{II}}}\,. \tag{56}$$

The iterative correction to the displacement increment $\delta \mathbf{u}_{i+1}$ can now be determined

from [*cf.* eqs. (52)-(54)]

$$\delta \mathbf{u}_{i+1} = \delta \mathbf{u}^{\mathrm{I}}_{i+1} + \Delta t_{i+1}\, \delta \mathbf{u}^{\mathrm{II}}_{i+1} \,. \tag{57}$$

The performance of the method is shown in Figures 5 and 6. In Figure 5 a simple shallow truss structure is shown composed of a visco-elastic material. Figure 6 gives the time-displacement diagram. We observe that when the structure stiffens, the time step is made smaller while the displacement increments remain constant.

6. References

Anderson, C.A., Bazant, Z.P., Buyukozturk, O., Jonasson, J.-E. and Willam, K. (1988) Finite element analysis of creep and shrinkage, in *Mathematical Modeling of Creep and Shrinkage of Concrete,* (ed. Z.P. Bazant), J. Wiley & Sons, Chichester, pp. 275-310.

Bazant, Z.P. and Wu, S.T. (1973) Dirichlet series creep function for aging concrete. *ASCE J. Eng. Mech. Div.*, 99, 367-387.

Bazant, Z.P. and Wu, S.T. (1974) Rate-type creep law of aging concrete based on Maxwell chain. *RILEM Materials and Structures*, 7, 45-60.

Bazant, Z.P., Dougill, J., Huet, C., Tsubaki, T. and Wittmann, F.H. (1988) Material models for structural creep analysis, in *Mathematical Modeling of Creep and Shrinkage of Concrete,* (ed. Z.P. Bazant), J. Wiley & Sons, Chichester, pp. 275-310.

van den Bogert, P.A.J., de Borst, R. and Nauta, P. (1987) Simulation of the mechanical behavior of young concrete. *IABSE Reports*, 54, 339-347.

de Borst, R. and Nauta, P. (1985) Non-orthogonal cracks in a smeared finite element model. *Eng. Comput.*, 2, 35-46.

de Borst, R. (1987) Smeared cracking, plasticity, creep and thermal loading - A unified approach. *Comp. Meth. Appl. Mech. Eng.*, 62, 89-110.

de Borst, R. (1989) Thermal stresses, in *Fracture Mechanics of Concrete Structures: From Theory to Applications,* (ed. L. Elfgren), Chapman and Hall, London and New York, pp. 148-154.

Brameshuber, W. and Hilsdorf, H.K. (1989) Development of strength and deformability of very young concrete, in *Fracture of Concrete and Rock* (eds. S.P. Shah and S.E. Swartz), Springer-Verlag, New York-Berlin-Heidelberg, pp. 409-421.

Crisfield, M.A. (1981) A fast incremental/iterative procedure that handles snap-through. *Comput. Struct.* 13, 55-62.

Hill, R. (1962) Acceleration waves in solids. *J. Mech. Phys. Solids*, 10, 1-16.

Ramm, E. (1981) Strategies for tracing the nonlinear response near limit points, in *Nonlinear Finite Element Analysis in Structural Mechanics,* (eds. W. Wunderlich, E. Stein and K.-J. Bathe), Springer-Verlag, Berlin, pp. 63-83.

Reinhardt, H.W., Blaauwendraad, J., Jongedijk, J. (1982) Temperature development in concrete structures taking account of state dependent properties. *Proc. Int. Conf. Concrete at Early Ages,* Paris.

Rice, J.R. (1976) The localization of plastic deformation, in *Theoretical and Applied Mechanics,* (ed. W.T. Koiter), North-Holland, Amsterdam, pp. 207-220.

Riks, E. (1979) An incremental approach to the solution of snapping and buckling problems. *Int. J. Solids Structures*, 15, 529-551.

Rots, J.G. (1988) *Wave Propagation, Computational Modelling of Concrete Fracture.* Dissertation, Delft University of Technology, Delft.

Sluys, L.J. (1992) *Wave Propagation, Localisation and Dispersion in Softening Solids.* Dissertation, Delft University of Technology, Delft.

Taylor, R.L., Pister, K.S. and Goudreau, G.L. (1970) Thermomechanical analysis of viscoelastic solids. *Int. J. Num. Meth. Eng.*, 2, 45-60.

Zienkiewicz, O.C., Watson, M. and King, I.P. (1968) A numerical method of viscoelastic creep analysis. *Int. J. Mech. Sci.*, 10, 807-827.